Journal of Magnetism and Magnetic Materials 473 (2019) 21–25

Contents lists available at ScienceDirect

Journal of Magnetism and Magnetic Materials

journal homepage: www.elsevier.com/locate/jmmm

Research articles

The use of magnetic targeting for drug delivery into cardiac myocytes

Byung-Kwan Lim[a], Elyse C. Tighe[b], Seong Deok Kong[b,*]

[a] Department of Biomedical Science, Jungwon University, Goesan-gun 28024, South Korea
[b] Department of Bioengineering, Gordon and Jill Bourns College of Engineering, California Baptist University, CA 92504, United States

ARTICLE INFO

Keywords:
Cardiac myocytes
External magnetic fields
Magnetic nanoparticle drug delivery
Magnetic-field guided

ABSTRACT

With the continuous technological advancements being made in the medical field every day, the ability to improve drug delivery uptake in cardiac research is a prominent topic of discussion. Nanoparticles provide the opportunity to improve the efficiency of drug therapy while minimizing chemotherapy side effects through controllably releasing the encapsulated drug at the target site. Mono-disperse Fe_3O_4 nanoparticles/polystyrene composite nanospheres with a large volume fraction of trapped magnetite and fluorophores were used in an *in vivo* experiment. In this study, magnetic nanoparticles were successfully delivered into the heart by utilizing magnetic targeting. Magnetic targeting allowed the mono-disperse Fe_3O_4 nanospheres to be dramatically localized in the heart myocardium. This increased the quantity of delivery to the cardiac myocytes in comparison to magnetic nanospheres without magnetic targeting.

1. Introduction

The heart is the center of a vast network of arteries, veins, capillaries, and blood vessels that function to supply the entire human anatomy with essential blood and oxygen [1,2]. When medical issues arise, this network provides a perfect transportation system for drug treatment. Recently new information on cardiac targeted drug delivery has begun to show a strong limitation that has affected medical breakthroughs from occurring [3,4]. Cardiac myocytes continuously contract while maintaining an intact membrane structure. As a result to its' differences in comparison to other cell types, drug delivery efficiency has been shown to be significantly lower [3,5–8]. Using this limitation as motivation, it is essential to develop a new drug delivery strategy to improve the medical treatment and patient outcome for those living with advanced heart diseases. Previous studies have shown that intramyocardial injection is a useful technique to deliver therapeutic drug to the ischaemically-damaged heart [9–11]. Due to the invasiveness of the technique and surgical intervention required, the use of intramyocardial injection has been shown to be limited in clinical settings [5,8]. As a result, intravenous injection has been widely used in animal models and patient. While an issue itself, the major dilemma with intramyocardial injection is its' systemic infusion tendency to be low targeting therapy. In normal cases, most delivered drugs go through detoxification in the liver. This results in only a fraction of the infused drug successfully reaching the target heart muscle. As a potential solution to this problem, magnetic nanoparticles have the potential to be designed to circumvent this clearance. Nanoparticle-based molecular transport has been proven to enhance drug delivery in cardiology fields of research [12–14]. Specially, Mono-disperse Fe_3O_4 nanoparticles/polystyrene composite nanospheres with a large volume fraction of trapped magnetite have shown promising results for deep tumor delivery by applying an external Direct Current (DC) magnetic field [15]. These advancements provide the ability of researchers to predict and control the release using a remote radio frequency (RF) magnetic fields provides a significant advantage in drug delivery [16]. Previously we presented a hollow silica nanocapsule capable of deep tumor delivery with applying DC magnetic field and on–off switchable drug release via application of a RF magnetic field [15].

In this study, the magnetic nanoparticle feasibility of delivering to the heart by external magnetic field was verified. As shown in the data, magnetic vectored nanoparticle dramatically localized in the heart myocardium by magnetic field guidance. Using these results as evidence, we strongly believe that it should be studied further as a strategy for drug delivery into the intact heart.

2. Materials and methods

2.1. General comments

All reagents were purchased from Sigma-Aldrich, Inc. and Alfa Aesar, and used without further purification. The microscopy characterization of synthesized magnetic nanoparticles was carried out

* Corresponding author.
E-mail address: skong@calbaptist.edu (S.D. Kong).

https://doi.org/10.1016/j.jmmm.2018.09.118
Received 23 June 2018; Received in revised form 17 September 2018; Accepted 28 September 2018
Available online 29 September 2018
0304-8853/

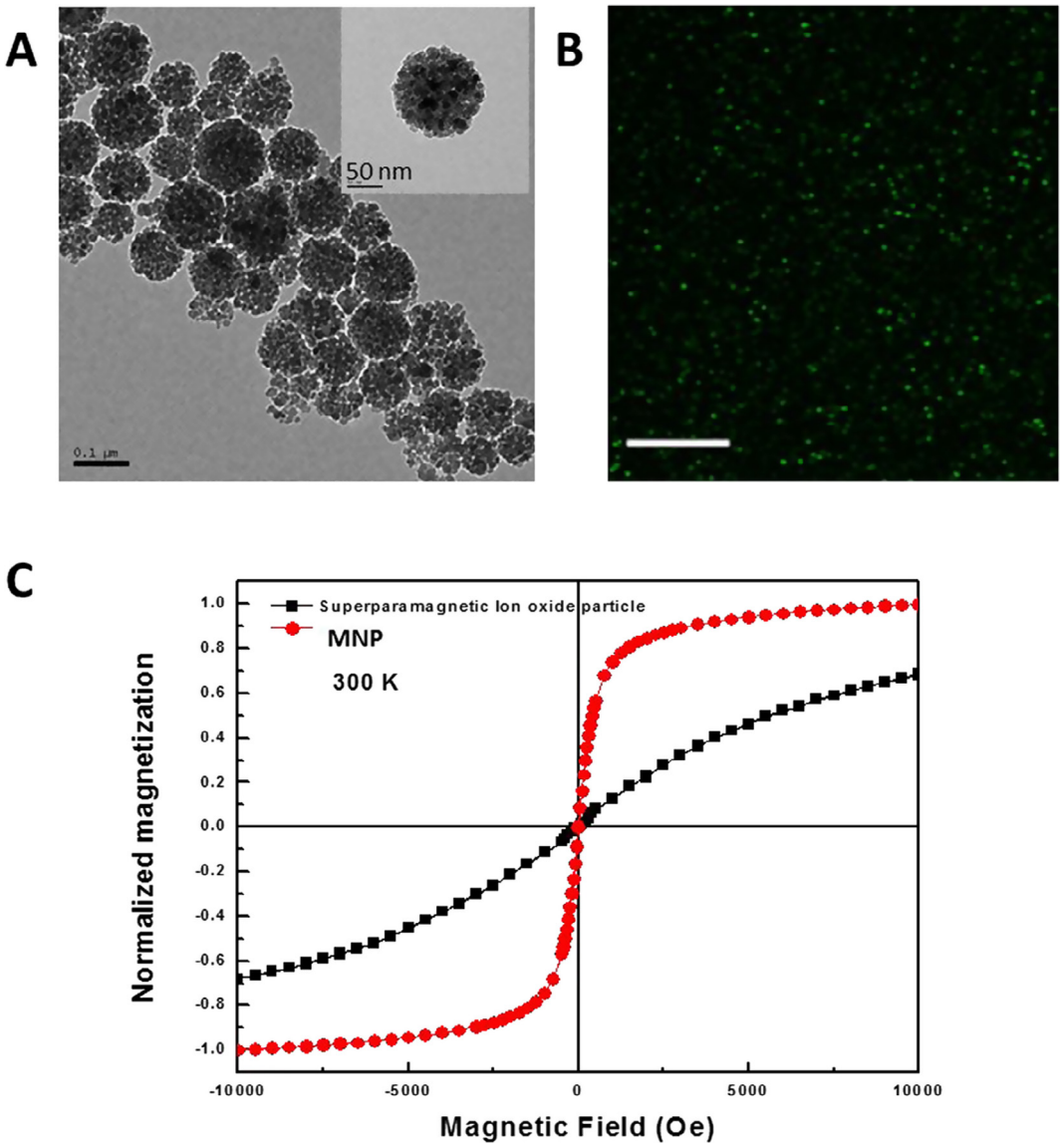

Fig. 1. Characterization of fluorophore labeled magnetic nanoparticles (MNPs). (A) TEM micrograph showing trapped magnetic nanoparticles in MNPs-scale bar: 100 nm (inset) Clear sphere shape with trapped 10 nm Fe_3O_4 nanoparticles – scale bar: 50 nm. (B) Confocal microscopy images of MNPs (green colored fluorophore, 9,10-bis(phenylethynyl)anthracene, in MNPs)-scale bar: 50 μm. (C) M − H loops showing a significant increase in magnetic moment in MNP configuration as compared with isolated 10 nm magnetic nanoparticles of Fe_3O_4.

using a transmission electron microscope (FEI Tecnai G2 Sphera with 200 kV accelerated voltage). Magnetic measurement was performed using SQUID magnetometer (Quantum Design MPMS2).

2.2. Synthesis of mono-disperse Fe_3O_4 nanoparticles/polystyrene composite nanospheres with a large volume fraction of trapped magnetite and fluorophores

All Fe_3O_4 nanoparticles/polystyrene composite nanospheres were prepared by combining mini-emulsion/emulsion polymerization technique according to the previous reported paper in our lab [15]. Briefly, a mixture of 24 g $FeCl_3{\cdot}6H_2O$ and 9.82 g $FeCl_2{\cdot}4H_2O$ was stirred with 50 mL of ammonium hydroxide under nitrogen gas at 80 °C, and then the solution was reacted for 1.5 h after the addition of 3.76 g of oleic acid. The magnetite nanoparticles fabricated were washed with deionized water 3 or 4 times to make them neutral pH and then were transferred in situ in octane. Magnetite and styrene mini emulsion containing 9,10-bis(phenylethynyl)anthracene were prepared using ultrasound and a microporous glass membrane. With these emulsions, mono disperse Fe_3O_4/polystyrene nanospheres were synthesized with 40 mg potassium peroxydisulfate (KPS) at 80 °C for 20 h reaction time. The synthesized magnetic nanoparticles (MNPs) were centrifuged and then were redispersed into 0.5% (wt/vol) polyoxyethylenesorbitanmonolaurate aqueous solution.

2.3. Mouse neonatal cardiac myocytes culture

Neonatal cardiac myocytes were cultured by 1–2 day neonatal mice heart, each mice heart was collected and digested by 0.25% trypsin-EDTA solutions at 4 °C for overnight. The next day, the hearts were digested by type2 collagenase (2 mg/ml) at 37 °C for 30 min. Single myocytes were isolated from each digested heart by pipetting and then cultured with a 0.1% gelatin coated culture plate. A humidified atmosphere at 37 °C containing 5% of CO_2, was used to culture $5x10^4$ cells in a myocytes culture medium (DMEM medium:M199 medium = 3:1 mixed, Invitrogen, CA, USA) containing 10% fetal bovine serum (FBS; inactivated at 56 °C for 30 min; Invitrogen, USA), 5% horse serum, 100 μ/ml Penicillin/Streptomycin until the isolated cardiac myocyte cells

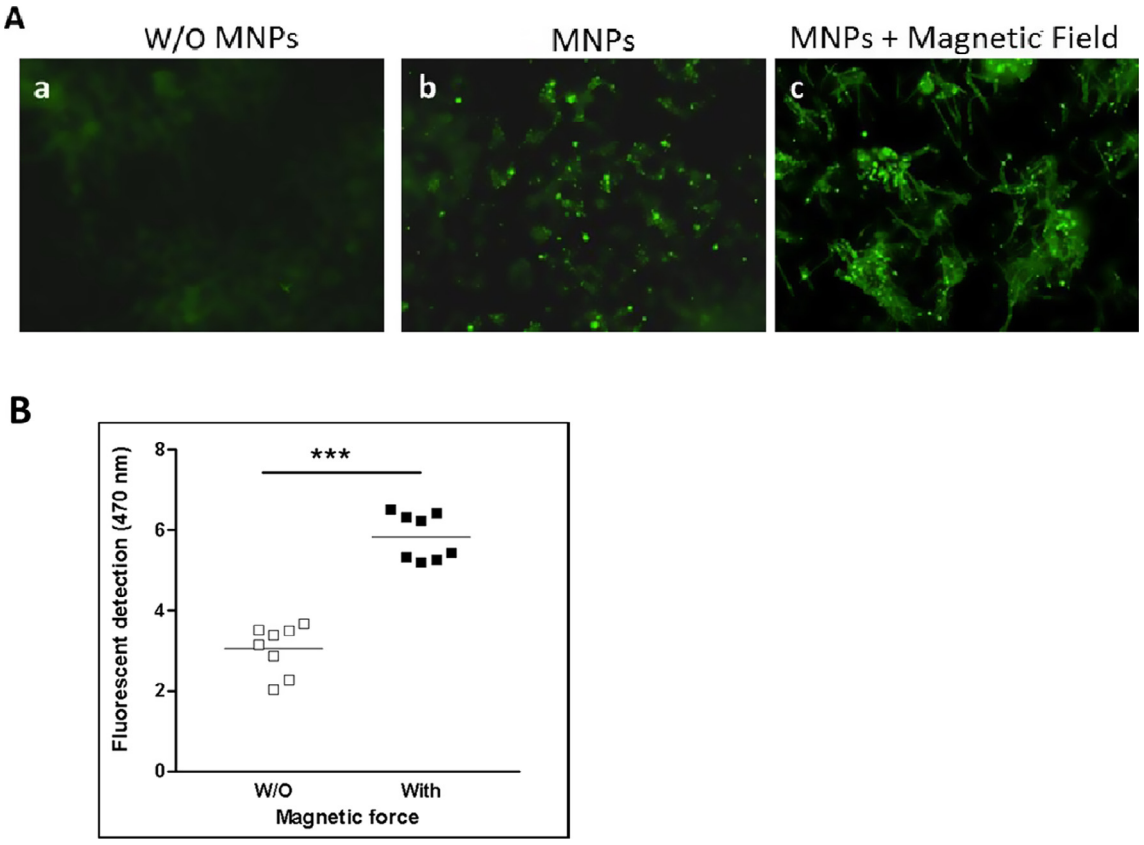

Fig. 2. Nanoparticle can penetrate into neonatal cardiac myocyte. (A) A comparison of the images of the magnetic force induced nanoparticle delivery into myocardium (a) without nanoparticles (b) with nanoparticles (c) nanoparticles and magnetic field. (X200 magnification) (B) Fluorescent detection with and without a magnetic field application. All data in this figure are the means ± s.e.m. from 3 independent experiments. $^{***}P < 0.001$.

that were cultured in the plate became attached [17]. MNPs were added into the cardiac myocytes cultured plate and then a magnetic field was applied to the cultured plate for 30 min. At the end of incubation, cells were thoroughly washed in warm HEPES buffered saline solution (5 times, 5 min each) to remove any free particles from the cell surface. An inverted-fluorescent microscope was used to observe nanoparticle penetration. To measure the amount of uptake nanoparticle, the cardiac myocytes were lysed by phosphate-buffered saline (PBS) containing 0.1% Tween20. Cell lysed supernatant was added into a black 96-well reading plate and then fluorescence was measured using a microplate reader (Molecular Devices LLC, Downingtown, PA, USA) at a wavelength of 405 nm.

2.4. Nanoparticle tail intra-vein injection

The efficiency of nanoparticle uptake into the mice hearts was assessed by injecting magnetic nanoparticles in the tail veins. 8 week male Balb/C mice were intravenously injected using $2x10^6$ nanoparticles in 100 μl saline. In order to demonstrate that the nanoparticles move well in an aqueous solution, in the presence of an applied field of about 500 Oe, the particles moved a distance of ~1.5 cm from a permanent magnet placed nearby [15]. The nanoparticles exhibited a superior magnetic vector with a movement speed of ~0.24 cm/s. The magnetic field applied was ~900 Oe at a distance of 1 cm and a distance of 2 cm when ~280 Oe was applied. A Nd–Fe–B disk-shaped magnet (1 in. diameter × 0.5 in. thick, Dexter Magnetic Technologies with a magnetic field strength on the surface measured by gauss meter of 6.3 KOe) was placed outside of the mouse chest on the surface of the mouse skin. After 1 h incubation, both mice with or without magnetic fields around the chest were euthanized intraperitoneal with Ketamine (60 mg/kg bodyweight)/Xylazin (10 mg/kg) and then the heart, liver, and spleen were collected. For 2 h at 30% sucrose incubation the tissue was snap-frozen by embedding in OCT tissue Tek (Sakura Finetechnical, Torrance, CA) [17]. All procedures were carried out in accordance with guidelines set by the UCSD Institutional Animal Care Program (ACP) and were approved by the IACUC.

2.5. Heart fluorescent detection

Hearts were snap-frozen by embedding in OCT Tissue Tek using isobutane chilled in dry ice. 7-μm sections were cut by Leica cryostat (Leica, Bannockburn, IL). Specimens were fixed with ice-cold acetone then mounted by anti-bleaching mounting solution (BD science, USA). Fluorescence images were taken and processed by fluorescent microscope. Nanoparticle uptake levels were quantified with Image J (NIH, Bethesda, ML) densitometry based on signal intensity.

2.6. Statistical analysis

Data values were expressed as mean ± SEM unless otherwise noted. Statistical significance was evaluated using the unpaired Student's *t*-test for comparisons between 2 means. P-values < 0.05 were considered as significantly different [17].

3. Results and discussion

3.1. Characterization of fluorophore labeled magnetic nanoparticles (MNPs)

9,10-bis(phenylethynyl)anthracene green fluorophore-embedded MNPs of ~100 nm diameter (average size of MNPs = 97 ± 8.2 nm, supplement data Fig. S2) were developed using a modified emulsion

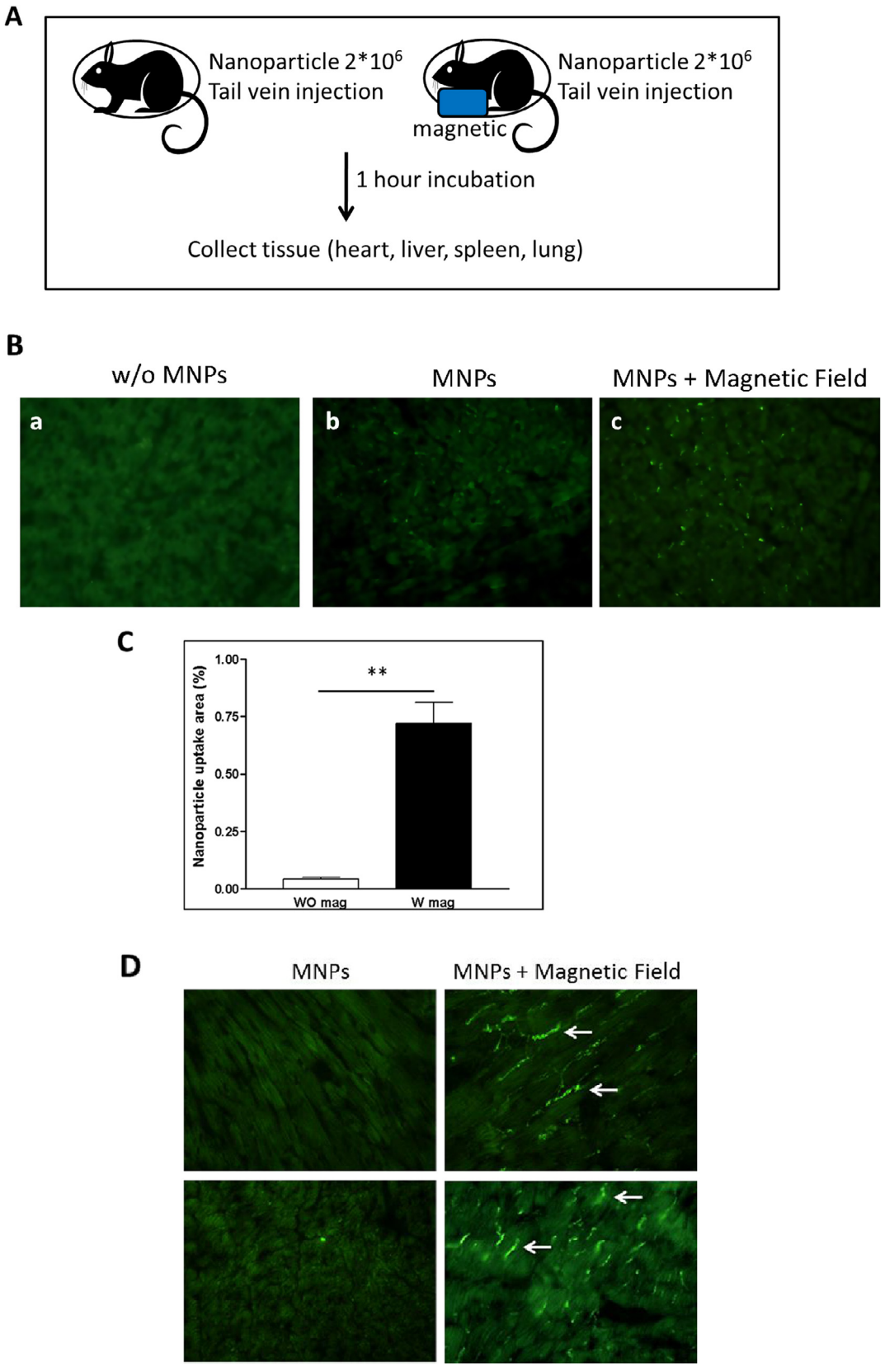

Fig. 3. Magnetic force induce nanoparticle delivery into myocardium. (A) Schematic illustration of incubation and MNPs intravein injection of mice tail. (B) Comparison images of accumulation of MNPs in myocardium cells in the tissue at a magnification of ×200. (×200 magnification) (C) Nanoparticle uptake with and without magnetic field application. (D) Comparison images of accumulation of MNPs in myocardium cells in the tissue at a magnification of ×400 Figures B and D are the same isolated myocardium cells, but were taken at different magnifications. The increase in magnification in figure D provides clear images that there was an increase in MNP accumulation deep within the tissue. All data in this figure are the means ± s.e.m. from 3 independent experiments performed (n = 3 each group). $^{**}P < 0.01$.

process for imaging MNPs [18]. Fig. 1 shows that MNPs are 100 nm spheres containing lots of 10 nm super-paramagnetic Fe_3O_4 magnetite beads (Fig. 1A), and representative micrographs and fluorescent images of MNPs by laser scanning con-focal microscopy (LSCM) (Fig. 1B). The M−H magnetization loop of the MNPs was compared with the free 10 nm magnetite of same individual particle size (~10 nm) (Fig. 1C), which provided substantially improved magnetization (~5 times higher at 500 Oe) compared to typical super-paramagnetic iron oxide nanoparticles. This was attributed to their close proximity and tighter interaction of magnetic particles in the confined geometry of polystyrene particles resulting in the higher magnetization and enhanced response to applied magnetic field [18].

3.2. Nanoparticle penetration into cultured neonatal cardiac myocyte

Magnetic vectored nanoparticles were generated and added into cultured neonatal cardiac myocytes well plate to confirm whether a magnetic force can improve a nanoparticle's penetration into cultured cardiac myocytes. There is a limitation to the extent of delivery of genes or drugs into cultured cardiac myocytes, with < 2% cell delivery by the liposome transfection method [19]. Our results showed that nanoparticles are able to penetrate into cardiac myocytes by themselves without cytotoxicity. However, many particles just attached to the outside of the cell's surface without magnetic field (Fig. 2A and b).

In contrast, a magnetic field significantly increased the magnetic vectored nanoparticle penetration into cardiac myocytes. Nanoparticles can be delivered into thin muscle fiber with assistance from a magnetic field (Fig. 2A and C). Inside uptake of nanoparticles was measured by a fluorescent micro-plate reader. The magnetic field significantly increased nanoparticle uptake into cardiac myocytes (Fig. 2B). This result indicated that magnetic embedding helps facilitate the regulation of nanoparticle penetration into target cell or tissue.

3.3. Nanoparticle delivery to the heart

Nanoparticle delivery on the heart was confirmed by *in vivo* accumulation experiments using mice with or without magnetic field treatment. Mice were infused with 2×10^6 per 100 μl PBS of green colored fluorophore, 9,10-bis(phenylethynyl)-anthracene,-tagged magnetic nanoparticle. Mice were then immobilized and treated with a magnet placed in contact with the epidermis of the mice near the chest area. After a constant magnetic field was applied for one hour, they were euthanized and the tissue samples were analyzed (Fig. 3A). As shown in Fig. 3B, the myocardium accumulation of nanoparticle is miniscule with no magnetic field applied. In contrast, the hearts of the mice treated with a magnetic field indicated that nanoparticle accumulation at the myocardium cell to cell junction was significantly increased as compared to the control group sample (magnetic nanoparticle similarly injected tail-vein injected but no magnetic field applied) (Fig. 3B and D). The mean ± SEM bar graph and statistical significance $P < 0.01$ are marked on the figure (Fig. 3C). In addition, the nanoparticles accumulated deeper into the cardiac intercalated discs with magnetic field application compared to the control sample. Fig. 3D clearly shows that magnetic nanoparticles are present deep within the tissue structure compared to those where no magnetic targeting was applied. The results in this paper clearly showed that a magnetic nanoparticle is a simple but powerful way of targeted drug delivery into the heart myocardium. Magnetic field application significantly improved nanoparticle accumulation into the intact heart intercalated discs. Moreover, the amount of nanoparticle accumulation to other organs was minimized (supplement data, Fig. S1).

4. Conclusion

Through completion of this study, the ability of magnetic nanoparticles to accumulate in targeted areas of mice was successfully demonstrated. The use of a magnetic field over the heart myocardium in mice significantly increased the localization of nanoparticles. In addition, the nanoparticle uptake area showed an overwhelming increase for magnetic field (MF) application in comparison to nanoparicle injection without MF application. The use of magnetic fields increased the uptake 15 times more than the no use of magnetic fields.

Acknowledgment

This work was supported by the mini-grant of California Baptist University.

Appendix A. Supplementary data

Supplementary data to this article can be found online at https://doi.org/10.1016/j.jmmm.2018.09.118.

References

[1] D. Lloyd-Jones, R.J. Adams, T.M. Brown, M. Carnethon, S. Dai, G. De Simone, T.B. Ferguson, E. Ford, K. Furie, C. Gillespie, A. Go, K. Greenlund, N. Haase, S. Hailpern, P.M. Ho, V. Howard, B. Kissela, S. Kittner, D. Lackland, L. Lisabeth, A. Marelli, M.M. McDermott, J. Meigs, D. Mozaffarian, M. Mussolino, G. Nichol, V.L. Roger, W. Rosamond, R. Sacco, P. Sorlie, R. Stafford, T. Thom, S. Wasserthiel-Smoller, N.D. Wong, J. Wylie-Rosett, Executive summary: heart disease and stroke statistics–2010 update: a report from the American Heart Association, Circulation 121 (7) (2010) 948–954.

[2] F. Bosetti, Z.S. Galis, M.S. Bynoe, M. Charette, M.J. Cipolla, G.J. Del Zoppo, D. Gould, T.S. Hatsukami, T.L. Jones, J.I. Koenig, G.A. Lutty, C. Maric-Bilkan, T. Stevens, H.E. Tolunay, W. Koroshetz, Small, blood vessels: big health problems?": scientific recommendations of the National Institutes of Health Workshop, J. Am. Heart Assoc. 5 (11) (2016).

[3] D. Lloyd-Jones, R.J. Adams, T.M. Brown, M. Carnethon, S. Dai, G. De, Simone, T.B. Ferguson, E. Ford, K. Furie, C. Gillespie, A. Go, K. Greenlund, N. Haase, S. Hailpern, P.M. Ho, V. Howard, B. Kissela, S. Kittner, D. Lackland, L. Lisabeth, A. Marelli, M.M. McDermott, J. Meigs, D. Mozaffarian, M. Mussolino, G. Nichol, V.L. Roger, W. Rosamond, R. Sacco, P. Sorlie, T. Thom, S. Wasserthiel-Smoller, N.D. Wong, J. Wylie-Rosett, Heart disease and stroke statistics–2010 update: a report from the American Heart Association, Circulation 121 (7) (2010) e46–e215.

[4] W.H. Barker, J.P. Mullooly, W. Getchell, Changing incidence and survival for heart failure in a well-defined older population, 1970–1974 and 1990–1994, Circulation 113 (6) (2006) 799–805.

[5] J.A. Mariani, D.M. Kaye, Delivery of gene and cellular therapies for heart disease, J. Cardiovasc. Transl. Res. 3 (4) (2010) 417–426.

[6] K. Ishikawa, L. Tilemann, K. Fish, R.J. Hajjar, Gene delivery methods in cardiac gene therapy, J. Gene Med. 13 (10) (2011) 566–572.

[7] W.J. Geldenhuys, M.T. Khayat, J. Yun, M.A. Nayeem, Drug delivery and nanoformulations for the cardiovascular system, Res. Rev. Drug Deliv. 1 (1) (2017) 32–40.

[8] M. Liu, M. Li, G. Wang, X. Liu, D. Liu, H. Peng, Q. Wang, Heart-targeted nanoscale drug delivery systems, J. Biomed. Nanotechnol. 10 (9) (2014) 2038–2062.

[9] S. Fukushima, A. Varela-Carver, S.R. Coppen, K. Yamahara, L.E. Felkin, J. Lee, P.J. Barton, C.M. Terracciano, M.H. Yacoub, K. Suzuki, Direct intramyocardial but not intracoronary injection of bone marrow cells induces ventricular arrhythmias in a rat chronic ischemic heart failure model, Circulation 115 (17) (2007) 2254–2261.

[10] P.M. Grossman, Z. Han, M. Palasis, J.J. Barry, R.J. Lederman, Incomplete retention after direct myocardial injection, Catheter. Cardiovasc. Interv. 55 (3) (2002) 392–397.

[11] C. Schneider, K. Jaquet, R. Malisius, S. Geidel, E. Bahlmann, S. Boczor, T. Rau, M. Antz, K.H. Kuck, K. Krause, Attenuation of cardiac remodelling by endocardial injection of erythropoietin: ultrasonic strain-rate imaging in a model of hibernating myocardium, Eur. Heart J. 28 (4) (2007) 499–509.

[12] Y. Zhang, W. Li, L. Ou, W. Wang, E. Delyagina, C. Lux, H. Sorg, K. Riehemann, G. Steinhoff, N. Ma, Targeted delivery of human VEGF gene via complexes of magnetic nanoparticle-adenoviral vectors enhanced cardiac regeneration, PLoS One 7 (7) (2012) e39490.

[13] W. Li, N. Ma, L.L. Ong, A. Kaminski, C. Skrabal, M. Ugurlucan, P. Lorenz, H.H. Gatzen, K. Lutzow, A. Lendlein, B.M. Putzer, R.K. Li, G. Steinhoff, Enhanced thoracic gene delivery by magnetic nanobead-mediated vector, J. Gene Med. 10 (8) (2008) 897–909.

[14] E. Delyagina, W. Li, N. Ma, G. Steinhoff, Magnetic targeting strategies in gene delivery, Nanomedicine (Lond.) 6 (9) (2011) 1593–1604.

[15] S.D. Kong, W. Zhang, J.H. Lee, K. Brammer, R. Lal, M. Karin, S. Jin, Magnetically vectored nanocapsules for tumor penetration and remotely switchable on-demand drug release, Nano Lett. 10 (12) (2010) 5088–5092.

[16] J.P. Smith, Nanoparticle delivery of anti-tuberculosis chemotherapy as a potential mediator against drug-resistant tuberculosis, Yale J Biol Med. 84 (4) (2011) 361–369.

[17] B.K. Lim, A.K. Peter, D. Xiong, A. Narezkina, A. Yung, N.D. Dalton, K.K. Hwang, T. Yajima, J. Chen, K.U. Knowlton, Inhibition of Coxsackievirus-associated dystrophin cleavage prevents cardiomyopathy, J. Clin. Invest. 123 (12) (2013) 5146–5151.

[18] S.D. Kong, J. Lee, S. Ramachandran, B. Eliceiri, V.I. Shubayev, R. Lal, S. Jin, Magnetic targeting of nanoparticles across the intact blood-brain barrier, J. Control. Release 164 (2012) 49–57.

[19] Y. Sawa, K. Suzuki, H.Z. Bai, R. Shirakura, R. Morishita, Y. Kaneda, H. Matsuda, Efficiency of in vivo gene transfection into transplanted rat heart by coronary infusion of HVJ liposome, Circulation 92 (9) (1995) 479–482.